

TeV neutrinos from core collapse supernovae and hypernovae

Soebur Razzaque,¹ Peter Mészáros^{1,2,3} and Eli Waxman⁴¹ Department of Astronomy & Astrophysics, Department of Physics, Pennsylvania State University, University Park, PA 16802, USA² Institute for Advanced Study, Princeton, NJ 08540, USA³ Department of Atomic Physics, Eötvos University,

Hungarian Academy of Sciences, Budapest, Hungary

⁴ Physics Faculty, Weizmann Institute of Science, Rehovot 76100, Israel

(Dated: January 28, 2020)

A fraction of core collapse supernovae of type Ib/c are associated with gamma-ray bursts, which are thought to produce highly relativistic jets. Recently, it has been hypothesized that a larger fraction of core collapse supernovae produce slower jets, which may contribute to the disruption and ejection of the supernova envelope, and explain the unusually energetic hypernovae. We explore the TeV neutrino signatures expected from such slower jets, and calculate the expected detection rates with upcoming Grigatov Cherenkov experiments. We conclude that individual jetted SNe may be detectable from nearby galaxies.

PACS numbers: 97.60.Bw, 96.40.Tv, 98.70.Sa

Core collapse supernovae (SNe) are known sources of 1–10 M eV neutrinos, as detected from SN 1987A [1]. Previously, 100 TeV neutrinos were predicted from protons accelerated in internal shocks in relativistic jets associated with gamma-ray burst (GRB) event [2], independently of any SN connection. Long duration (& several seconds) GRBs are now known, in several cases, to be associated with SN type Ib/c events triggered by a stellar core collapse which is contemporaneous with the GRB event [3]. The relativistic jets from such core collapses are expected to produce a TeV neutrino precursor burst, while the jet is making its way out of the collapsing stellar progenitor [4], and this may be present even if the jet does not manage to burrow through the stellar envelope, i.e. choked bursts which are bright, but dark. These previous TeV neutrino predictions assumed jets, with bulk Lorentz factors $\gamma_b \approx 100$. The frequency of highly relativistic jets in SN like events is at most comparable to the ratio of GRBs to the average core-collapse SN events, $\sim 10^{-3}$.

The deposition of bulk kinetic energy from a jet into the stellar envelope may be a powerful contributor to the triggering of a core collapse SN or SN Ib/c [5] and/or to the disruption of the envelope [6]. Only a small fraction of core-collapse SNe appear to be associated with GRBs [7]. However, a significantly larger fraction of SNe may be endowed with slower jets, of γ_b few [6, 8, 9, 10], which may also give rise to "orphan" radio afterglows not associated with detected -ray emission [11]. In this Letter, we point out that SNe endowed with slow jets will be detectable sources of multi-GeV to TeV neutrinos. Since the occurrence rate per galaxy of SNe is much larger than for GRBs, the chances of one occurring nearby is significantly enhanced. Hyperenergetic SNe (hypernovae) will be fewer in number (10% of type Ib/c rate [12]), but will have a higher neutrino flux. We calculate the neutrino fluence from such slow-jet SNe within the nearest 20

Mpc, and the corresponding neutrino detectability with upcoming kilometer scale Cherenkov detectors in Antarctica and in the Mediterranean [13].

Jet dynamics. We take a jet, with $\gamma_b = 10^{0.5}$, inside the SN progenitor star. The corresponding jet opening angle is $\theta_j = 1^\circ$. With a variability time $t_v = 0.1t_{j,1}$ s at the jet's base, internal shocks occur in the jet at a collision radius $r_j = 2^{2/3}ct_v = 10^{10.8} \text{ cm}$, which is inside the progenitor star (typically a Wolf-Rayet star of 10^{11} cm radius for a SN Ib, or larger for other type II SN). Typical jet energy, inferred from GRBs, is $E_j = 10^{51.5} \text{ ergs}$ while inside the progenitor star. By analogy with the GRB case, we assume that a fraction $\eta_e = 0.1$ of E_j is converted into relativistic electron kinetic energy in the internal shocks, which then synchrotron radiate in the presence of magnetic fields representing a fraction $\eta_b = 0.1$ of E_j .

The volume number density of leptons and baryons present in the jet is $n_e^0 = n_p^0 = E_j = (2^{2/3}m_p c^3 t_{j,1})^{10^{20.5}} E^{51.5} \text{ cm}^{-3}$ in the comoving frame of the jet. Here $t_{j,1} = 10t_{j,1}$ s is the typical jet duration. Electrons and protons are expected to be accelerated to high energy in the internal shocks. Typically all electrons cooldown by synchrotron radiation within the dynamical time scale $t_{dyn}^0 = t_v = 1$ s. However, due to the large Thomson optical depth ($\tau_{th} = 10^{6.6} E^{51.5} \text{ cm}^{-3} t_{j,1}^{-1} t_v^{-1}$), synchrotron photons in the jet thermalize to a black body temperature of $E^0 = [15(\sim c)^3 E_j]^{1/4} = (2^{4/3} r_j^2 c t_j)^{1/4} = 4.3 E^{51.5} \text{ eV}$. Also photons from the shocked stellar plasma do not diffuse into the jet as a result of the high τ_{th} . The volume number density of thermalized photons produced by the shocks is $n^0 = E_j \eta_e = (2^{2/3} c E^0 t_j)^{1/2} = 10^{24.8} E^{3/4} \eta_e^{3/4} \text{ cm}^{-3}$.

The magnetic field strength in the jet is given by $B^0 = 4E_j \eta_b = (r_j^2 c t_j)^{1/2} = 10^{8.5} E^{1/2} \eta_b^{1/2} \text{ G}$

in the comoving frame. The corresponding shock acceleration time for protons is $t_{\text{acc}}^0 = AE_p^0 = eB^0 10^{12} (E_p^0 = \text{GeV}) A_1 E_{51:5}^{1=2} \frac{1=2}{b; 1} \frac{2}{b; 0.5} t_{j;1}^{1=2} t_{v;1} \text{ s}$. The maximum proton energy is limited by requiring this time not to exceed t_{dyn}^0 or other possible proton cooling process time scales.

Proton cooling time scales. The Bethe-Heitler (BH) interaction $p + pe$ has a logarithmically rising cross section $\sigma_{\text{BH}} = r_p^2 f(28=9) \ln [2E_p^0 E^0 = (m_p m_e c^4)] 106=9 \text{ g}$. The e^+ pairs are produced at rest in the center of mass (cm) frame of the $p + pe$ collision. The energy lost by the proton in each interaction is given by $E_p^0 = 2m_e c^2 \frac{0}{\text{cm}}$, where $\frac{0}{\text{cm}} = (E_p^0 + E^0) = (m_p^2 c^4 + 2E_p^0 E^0)^{1=2}$ is the Lorentz boost factor of the cm in the comoving frame. The energy loss rate of the proton is given by $dE_p^0 = dt_{\text{BH}}^0 = n^0 c_{\text{BH}} E^0$. The corresponding proton cooling time is $t_{\text{BH}}^0 = E_p^0 = (dE_p^0 = dt_{\text{BH}}^0) = E_p^0 = (2n^0 c_{\text{BH}} m_e c^2 \frac{0}{\text{cm}})$ in the comoving frame.

Protons, in the presence of the same magnetic field which is responsible for the electron synchrotron losses, also suffer synchrotron losses, but over a longer time scale given by $t_{\text{syn}}^0 = 6 m_p^4 c^3 = (T_{\text{th}}^2 m_e^2 E_p^0 B^0)^2 3.8 (E_p^0 = \text{GeV})^1 E_{51:5}^{1=2} \frac{1}{b; 1} \frac{4}{b; 0.5} t_{j;1} t_{v;1}^2 \text{ s}$.

Protons can also transfer energy to photons by inverse Compton (IC) scattering, because of the significantly high photon density (n^0) in the shocks. The IC cooling time in the Thomson limit is given by $t_{\text{IC}, \text{Th}}^0 = 3m_p^4 c^3 = (4 T_{\text{th}} m_e^2 E_p^0 n^0) 3.8 (E_p^0 = \text{GeV})^1 E_{51:5}^{1=2} \frac{1}{b; 1} \frac{4}{b; 0.5} t_{j;1} t_{v;1}^2 \text{ s}$. In the Klein-Nishina (KN) limit, the IC cooling time is given by $t_{\text{IC}, \text{KN}}^0 = 3E_p^0 = (4 T_{\text{th}} m_e^2 c^5 n^0) 10^{10.5} (E_p^0 = \text{GeV}) E_{51:5}^{1=2} \frac{1=2}{b; 1} \frac{2}{b; 0.5} t_{j;1}^{1=2} t_{v;1} \text{ s}$. The Thomson and the KN limits apply for E_p^0 much less or greater than $m_p^2 c^4 = E^0 10^{5.3} E_{51:5}^{1=4} \frac{1=4}{b; 1} \frac{1=4}{b; 0.5} t_{j;1}^{1=4} t_{v;1}^2 \text{ GeV}$, respectively, in the comoving frame.

We have plotted the proton acceleration time and the different cooling times in the comoving frames as functions of the proton energy in Fig. 1. Note that the BH cooling time (long dashed line) and the synchrotron cooling time (short dashed line) are first longer and then shorter than the maximum proton acceleration time (thick solid line). The corresponding maximum proton energy can be roughly estimated, by equating the t_{syn}^0 to t_{acc}^0 , as $E_{\text{p, max}}^0 = 10^{6.3} A_1 E_{51:5}^{1=4} \frac{1=4}{b; 1} \frac{1=4}{b; 0.5} t_{j;1}^{1=4} t_{v;1}^2 \text{ GeV}$.

Pion and muon production and cooling. High-energy protons interact with thermal photons in the shocks to produce neutrinos dominantly through $p + pe \rightarrow n^+ + e^+ + e^-$ channel. The threshold proton energy at which this is $E_{\text{p, th}}^0 = 0.3 = E^0 10^{4.8} E_{51:5}^{1=4} \frac{1=4}{b; 1} \frac{1=4}{b; 0.5} t_{j;1}^{1=4} t_{v;1}^2 \text{ GeV}$ and the corresponding optical depth is $\tau_{\text{p}} = 10^{7.8} E_{51:5}^{3=4} \frac{3=4}{b; 1} \frac{2}{b; 0.5} t_{j;1}^{3=4} t_{v;1}^2$, both evaluated in the comoving frame. However, low-energy protons may also produce π^0 by interacting with photons from high-energy tail of the black body photon

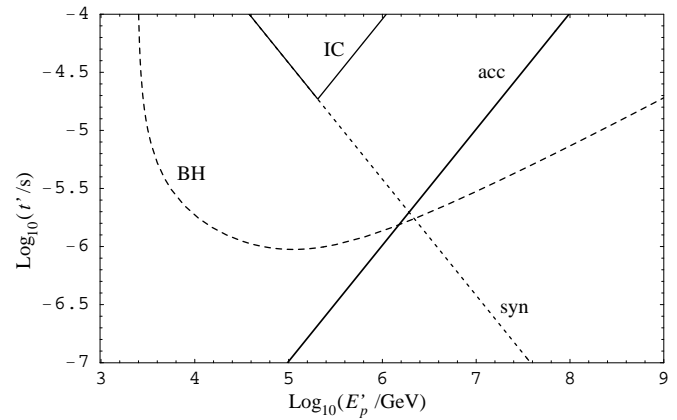


FIG. 1: Proton cooling time scales for different processes, in the comoving frame, as functions of energy. Also shown is the proton shock acceleration time. Burst parameters used are $E_{\text{sn}} = 10^{51.5} \text{ erg}$, $t_j = 10 \text{ s}$, $t_v = 10^{-1} \text{ s}$, $b = 3$, $e = b = 0.1$.

distribution until p falls below unity or below the optical depth for other processes such as proton-proton (pp) interaction. Similarly, protons with energy above $E_{\text{p, th}}^0$ interact with low energy photons to produce π^0 . pp interactions are effective at lower energy compared to $p + pe$ interactions. The total pion multiplicity from pp interactions is of the order unity in the energy range we are considering here [14]. For simplicity, we assume that each pp interaction produces single pion, the same as $p + pe$ interactions, down to the proton energy for which the corresponding neutrino energy is above detection threshold (E_{th}) on Earth. The available maximum proton energy to produce π^0 , through $p + pe$ interactions, is $E_{\text{p, max}}^0 = 10^{6.3} \text{ GeV}$.

High-energy pions and muons produced in $p + pe$ interactions do not all decay to neutrinos, as synchrotron radiation and IC scattering reduce the energy. The synchrotron break energies (below which pions and muons decay before undergoing significant cooling) are found by equating their synchrotron cooling times (t_{syn}^0) to their decay times (t_{dec}^0) in the comoving frame, which are $E_{\text{sb}}^0 = 10^2 E_{51:5}^{1=2} \frac{1=2}{b; 1} \frac{2}{b; 0.5} t_{j;1}^{1=2} t_{v;1}^2 \text{ GeV}$ and $E_{\text{sb}}^0 = 10^{0.7} E_{51:5}^{1=2} \frac{1=2}{b; 1} \frac{2}{b; 0.5} t_{j;1}^{1=2} t_{v;1}^2 \text{ GeV}$, respectively. Hence pions and muons in the energy range where they produce TeV neutrinos are already in the synchrotron suppression regime. In the case of IC scattering, muons suffer severe suppression both in the Thomson and in the KN regimes. In the case of pions, we define a suppression factor for neutrino production as

$$E^0 = \min(1; t_{\text{IC}}^0 / t_{\text{dec}}^0) = \frac{10^4 E^0}{10^{3.3}} \cdot 10^{2.2} \cdot E^0 = \text{GeV} \cdot 10^{3.66} \quad (1)$$

The neutrino flux from pion decay, which we calculate next, is suppressed by the factor E^0 .

Neutrino ux.] The observed isotropic equivalent proton uence from the SN jet, denoting the quantities in the observer's frame with subscript "ob", at a luminosity distance D_L , is $F_{p,ob} = E_{j,b}^2 (1+z) = (2 D_L^2 E_{p,ob}^2 \ln [E_{p,max} = E_{p,min}])$. Here we have assumed a shock accelerated proton energy distribution $/ E_p^2$. The energy and time in the observers frame and in the local rest frame (at red shift z) are related by $E_p = E_{p,ob} (1+z)$ and $t_j = t_{j,ob} = (1+z)$. The corresponding uence from proton interactions is

$$F_{,ob} = \frac{1}{4} \frac{4E}{b} \frac{E_{j,b}^2 (1+z)^3}{2 D_L^2 E^2 \ln [E_{p,min} = E_{p,max}]} \frac{E}{E_{,ob}} \quad (E_{p,min} \quad E_{p,max}) ; \quad (2)$$

per SN burst, assuming all shock accelerated protons convert to pions. We have also assumed that each neutrino carries one fourth of the pion energy which in turn carries 20% of the proton energy for both p and pp interactions. The neutrino energy range is then $E_{,ob,min} - E_{,ob,max} = E_{,th} - 0.05 b E_{p,max}^0 = (1+z) 10^{2.5} - 10^{5.5} = (1+z)$ GeV in the observer's frame on Earth. Here we have assumed $E_{,th} = 10^{2.5} E_{,2.5}$ GeV for a typical ice Cherenkov detector such as IceCube. For a SN at 20 Mpc ($D_L = 10^{25.8}$ cm, $z = 0$), e.g. in the Virgo cluster, the neutrino uence would be

$$F_{,ob} = \begin{cases} 10^{5.4} E_{,ob}^5 ; 10^{2.5} \cdot E_{,ob} = \text{GeV} \cdot 10^{3.56} \\ 10^{1.7} E_{,ob}^3 ; 10^{3.56} \cdot E_{,ob} = \text{GeV} \cdot 10^{5.5} \\ E_{51.5}^2 b_{0.5} D_{25.8}^2 ; \end{cases} \quad (3)$$

in units of GeV⁻¹ cm⁻² with $E_{,ob}$ measured in GeV.

To calculate the di use neutrino ux, we sum over uences from all slow-jet SNe distributed over cosmological distances in Hubble time. The SNe rate follows closely the star formation rate (SFR) which can be modeled as $\zeta(z) = 0.32 h_{70} \exp(3.4z) = [\exp(3.8z) + 45] M_{,yr}^{-1} M_{,pc}^{-3}$ per unit comoving volume [15]. Here $H_0 = 70 h_{70}$ km s⁻¹ Mpc⁻¹ is the Hubble constant. For a Friedmann-Robertson-Walker universe, the comoving volume element is $dV = dz = 4 D_L^2 c (1+z) dt = dz j$ and the relation between z and the cosmological time t is $(dt/dz)^{-1} = H_0 (1+z) / (1+z_m) (1+z)^2 / (2z + z^2)$. Here we have used the standard CDM cosmology with $z_m = 0.3$ and $z = 0.7$.

The number of SNe per unit star forming mass (f_{sn}) depends on the initial mass function and the SN threshold for stellar mass ($M = 8 M_{\odot}$). A Salpeter model (M) / M with different power-law indices can generate different values for f_{sn} , e.g. $0.0122 M^{-1}$ for $\alpha = 2.35$ [15] and $8 \cdot 10^{-3} M^{-1}$ for $\alpha = 1.35$ [16]. We adopt the model in Ref. [15] which corresponds to the local type II SNe rate $n_{sn}(z=0) = f_{sn} \zeta(z=0) = 1.2 \cdot 10^{-4} h_{70}^{-3} \text{yr}^{-1} M_{,pc}^{-3}$ agreeing with data [17].

The distribution of SNe per unit cosmological time and solid angle covered on the sky can be written as

$$\frac{d^2 N_{sn}}{dt d\Omega} = \frac{n_{sn}(z)}{4} \frac{dV}{dz} = \frac{n_{sn}(z) D_L^2 c}{(1+z)^2} \frac{dt}{dz} : \quad (4)$$

We assume a fraction $f_{sn} = 1$ of all SNe involve jets. The observed di use SNe neutrino ux, using Eq. (2), is then

$$\begin{aligned} \frac{d^2 N_{di}}{dt d\Omega} &= \int_0^{z_1} dz \frac{d^2 N_{sn}}{dt d\Omega} F_{,ob}(E_{,ob}) \\ &= \frac{c}{8} \frac{E_{j,b}^2}{E_{,ob}^2} \int_0^{z_1} dz \frac{n_{sn}(z) = (1+z)}{\ln [E_{,ob,max} = E_{,th}]} \\ &\quad \frac{dt}{dz} \frac{4E_{,ob} (1+z)}{b} \frac{E_{,ob} (1+z)}{E_{,ob}} \\ &\quad (E_{,th} \quad E_{,ob} \quad E_{,ob,max}) : \end{aligned} \quad (5)$$

We have plotted the di use ux from all cosmological slow-jet SNe in Fig. 2 by numerically integrating Eq. (5), assuming the maximum fraction $f_{sn} = 1$. Noting that the SFR peaks at $z = 1$, the changes of slope at $E_{,ob} = 10^{3.3}$ and $10^{5.2}$ GeV correspond to the change from the Thompson to the Klein-Nishina limit IC pion losses in Eq. (1), and to $E_{,ob} = 0.05 b E_{p,max}^0 = 2$, respectively. Also shown are the cosmological bounds (WB limits) on the di use neutrino ux [2], and the atmospheric ux from pion and kaon decays (conventional ux, [18]), compatible with AMANDA data [19].

$$\begin{aligned} \frac{8}{atm} &< \frac{0.012 E_{,ob}^{2.74}}{1 + 0.002 E_{,ob}} ; E_{,ob} < 10^{5.8} \text{ GeV} \\ &: \frac{3.8 E_{,ob}^{3.17}}{1 + 0.002 E_{,ob}} ; E_{,ob} > 10^{5.8} \text{ GeV} : \end{aligned} \quad (6)$$

Figure 2 demonstrates that the di use ux is unlikely to be detectable by km-scale telescopes. However, individual nearby SNe may be detectable, as we show below.

Neutrino event rate.] The effective area (A_e) of a Cherenkov detector depends on the zenith angle and the energy of the muon that is created by a charged current neutrino-nucleon (N) interaction in the vicinity of the detector. IceCube can trigger on muons of energy (which is 80% of the neutrino energy) above a few hundred GeV created within $A_e = 1 \text{ km}^2$ [13]. We assumed $E_{,th} = 300$ GeV, as discussed before. The angular sensitivity of the IceCube detector is 1 for muon tracks with $< 140^\circ$ zenith angles below 1 TeV. The pointing resolution gets better at higher energy.

The likeliest prospect for detection is from individual SNe in nearby starburst galaxies, such as M 82 and NGC 253 ($D_L = 3.2$ and 2.5 Mpc in the Northern and Southern sky, respectively), over a negligible background, using temporal and positional coincidences with optical detections. The SN rate in these is 0.1 yr^{-1} [20], much larger than in our own galaxy or in the Magellanic clouds.

To calculate the number of events in a km^2 detector such as IceCube, we use the uence of Eq.(3) from

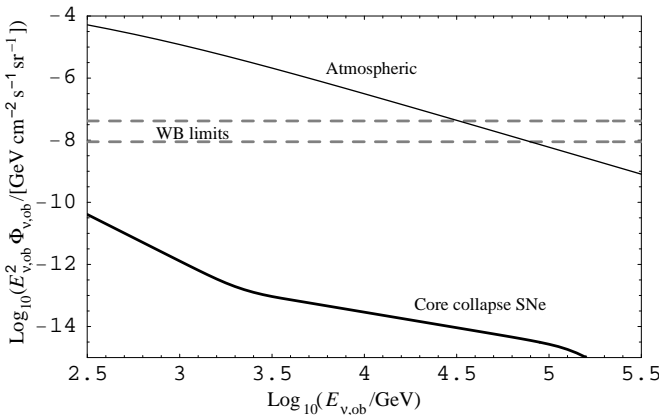


FIG. 2: Dismuon neutrino flux on Earth from all ($s_n = 1$, $E_j = 10^{51.5}$ erg) core collapse SNe (heavy solid curve). The dashed curves are the cosmic ray (WB) limits, and the light full curve is the atmospheric flux. This shows that the diisne flux is unlikely to be detectable with km^2 detectors. However, individual nearby SNe may be detectable, as discussed below.

each SN in the 300 GeV–300 TeV energy range, and the full detection probability depending on the source’s angular position. This probability depends on the Earth’s shadowing effect and the energy dependent N cross section inside A_e [21]. The number of events from M 82 and NGC 253 is $1.2 E_{51.5}$ and $2 E_{51.5}$; respectively per individual SN. The timing uncertainty in the optical detection of SN is 1 day. The corresponding atmospheric background events within 1 angular resolution is 0.07 for both M 82 and NGC 253 in the same energy range. At the quoted rate, a SN from one of these galaxies would be expected within five years. If these were hypernovae, where the kinetic energy is an order of magnitude larger, a direct scaling to $E_j = 10^{52.5}$ ergs would give 12 and 20 muon events respectively. Other nearby spirals (M 31, M 74, M 51, M 101, etc, and the Virgo cluster) will also contribute. At the standard rate of 1 SN yr^{-1} per 10^{10} blue solar luminosity for average galaxies, the roughly 4000 galaxies known within 20 Mpc would suggest a rate of 1 SN yr^{-1} .

Because of oscillations, neutrinos of all three flavors (ν_e , ν_μ , ν_τ) should reach us in equal proportion. However, only ν_e ’s are emitted from the sources under consideration and the total number of neutrino events (including ν_e and ν_τ) will remain the same as the ν_μ events we have calculated. The lack of good directional sensitivity for the ν_e and ν_τ events may prevent obtaining their positional coincidence with the SN. (Also, the A_e for ν_e and ν_τ detection are somewhat smaller than ν_μ .) However the timing coincidence of ν_e and ν_τ events with ν_μ events may still be useful to verify the neutrino oscillations at these energies, and test their common origin.

Discussion. While ultra-relativistic jets are thought to be responsible for the long-duration GRB associated with a small fraction of massive core collapse SNe, mildly relativistic jets may occur in a much larger (~ 1) fraction of core collapse SNe. Such slow jets may contribute to the bounce needed for ejecting the stellar envelope, resulting in the observed SN optical display. Late time (~ 1 yr) radio emission may be a signature of slow jets [11]. Such jets may also be needed to explain the apparent unusually large energies of hypernovae and the anisotropies inferred from optical polarization measurements of core collapse SNe. Here we propose, as an independent test of this model, the observation of TeV neutrinos, which may be detected in the near future with IceCube and other km^2 neutrino Cherenkov detectors.

We thank T. Abel, J. Bahcall, D. Cowen, A. Gal-Yam and C. Perna-Garay for helpful discussions. This work was supported by NSF AST 0098416, the Dennis H. Hungarica Scientiarum et Artium, the Monell Foundation, ISF and Minerva grants.

- [1] K. Hirata et al., *Phys. Rev. Lett.* **58**, 1490 (1987).
- [2] E. Waxman and J.N. Bahcall, *Phys. Rev. Lett.* **78**, 2292 (1997).
- [3] B. Zhang and P. Mészáros, *Int. J. Mod. Phys. A* **19**, 2385 (2004).
- [4] P. Mészáros and E. Waxman, *Phys. Rev. Lett.* **87**, 171102 (2001); S. Razzaque, P. Mészáros and E. Waxman, *Phys. Rev. D* **68**, 083001 (2003).
- [5] A. M. Korchlou, et al., *Astrophys. J.* **529**, L107 (1999).
- [6] A. I. Macfadyen, S.E. Woosley and A. Heger, *Astrophys. J.* **550**, 410 (2001).
- [7] E. Berger, et al., *Astrophys. J.* **599**, 408 (2003).
- [8] E. Waxman and A. Loeb, *Phys. Rev. Lett.* **87**, 071101 (2001).
- [9] E. Ramirez-Ruiz, A. Celotti and M. J. Rees, *Mon. Not. R. Astron. Soc.* **337**, 1349 (2002).
- [10] J. G. Ranot and A. Loeb, *Astrophys. J.* **593**, L81 (2003).
- [11] J. G. Ranot and E. Ramirez-Ruiz, *astro-ph/0403421*.
- [12] J.S. Bloom et al., *Astrophys. J.* **506**, L105 (1998); B. M. S. Hansen, *Astrophys. J.* **512**, L117 (1999).
- [13] J. Ahrens et al., *Astropart. Phys.* **20**, 507 (2004); E. A. Slatrides et al., *astro-ph/9907432*.
- [14] S. Razzaque, P. Mészáros and E. Waxman, *Phys. Rev. Lett.* **90**, 241103 (2003).
- [15] C. Porciani and P. Madau, *Astrophys. J.* **548**, 522 (2001).
- [16] L. Hernquist and V. Springel, *Mon. Not. R. Astron. Soc.* **341**, 1253 (2003).
- [17] P. Madau, M. della Valle and N. Panagia, *Mon. Not. R. Astron. Soc.* **297**, 17L (1998).
- [18] M. Thunman et al., *Astropart. Phys.* **5**, 309 (1996).
- [19] J. Ahrens, et al., *Phys. Rev. D* **66**, 012005 (2002).
- [20] A. A. Lobo-Herrero et al., *Mon. Not. R. Astron. Soc.* **325**, 1210A (2003).
- [21] S. Razzaque, P. Mészáros and E. Waxman, *Phys. Rev. D* **69**, 023001 (2004).